

Geometric Value Iteration: Dynamic Error-Aware KL Regularization for Reinforcement Learning

Toshinori Kitamura
Lingwei Zhu
Takamitsu Matsubara

KITAMURA.TOSHINORI.KT6@IS.NAIST.JP
ZHU.LINGWEI.ZJ5@IS.NAIST.JP
TAKAM-M@IS.NAIST.JP

Nara Institute of Science and Technology, Nara, JAPAN

Abstract

The recent boom in the literature on entropy-regularized reinforcement learning (RL) approaches reveals that Kullback-Leibler (KL) regularization brings advantages to RL algorithms by canceling out errors under mild assumptions. However, existing analyses focus on fixed regularization with a constant weighting coefficient and do not consider cases where the coefficient is allowed to change dynamically. In this paper, we study the dynamic coefficient scheme and present the first asymptotic error bound. Based on the dynamic coefficient error bound, we propose an effective scheme to tune the coefficient according to the magnitude of error in favor of more robust learning. Complementing this development, we propose a novel algorithm, Geometric Value Iteration (GVI), that features a dynamic *error-aware* KL coefficient design with the aim of mitigating the impact of errors on performance. Our experiments demonstrate that GVI can effectively exploit the trade-off between learning speed and robustness over uniform averaging of a constant KL coefficient. The combination of GVI and deep networks shows stable learning behavior even in the absence of a target network, where algorithms with a constant KL coefficient would greatly oscillate or even fail to converge.

Keywords: Geometric Policy Interpolation; Error-Awareness; KL Regularization; Reinforcement Learning

1. Introduction

The recently impressive successes of reinforcement learning (RL) rely heavily on the use of nonlinear function approximators such as deep networks (Mnih et al., 2015; Silver et al., 2017). However, the power of nonlinear approximators comes at a cost that approximation or estimation errors can easily go uncontrolled due to stochastic approximation using noisy samples (Fu et al., 2019), leading to performance oscillation or even divergent learning (Lillicrap et al., 2015; Fujimoto et al., 2018). While error propagation has been studied in detail in the literature of approximate dynamic programming (ADP) methods (Munos and Szepesvári, 2008; Scherrer et al., 2015), little is understood in the case of nonlinear approximation, such as whether the analyses in ADP still hold true. In practice, several empirical tricks like target networks or asynchronous updates need to be used to ensure stability and convergence for learning with deep networks (Mnih et al., 2015; Haarnoja et al., 2018).

The recent boom in the literature on entropy-regularized RL highlights the use of Kullback-Leibler (KL) divergence as a regularization term in the reward (Azar et al., 2012;

Kozuno et al., 2019; Vieillard et al., 2020a). It is known that by adding KL regularization, errors are *grouped* in the sense that they are accumulated as a summation (more details in Section 2). In standard L_p norm error propagation analysis, this summation is within the norm, as compared to the summation-over-norm of the standard ADP results (Bertsekas and Tsitsiklis, 1996; Munos and Szepesvári, 2008). Under mild assumptions such as the sequence of errors having martingale difference, the summation of errors asymptotically cancels out. This brings a great advantage to deep RL, where properly addressing errors is paramount (Fu et al., 2019; Fujimoto et al., 2018). However, there is a trade-off between learning speed and robustness in play since the policies change less between iterations with KL regularization. By setting the KL regularization coefficient as a constant, we lose the ability to dynamically trade-off speed and robustness, and hence the resultant algorithms might not be suitable for robustness-critical problems. In practice, wild performance oscillation can indeed be observed (Nachum et al., 2018), since summation is still sensitive to outliers and the errors at the early stage of learning are typically large.

In this paper, we propose dynamically adjusting the KL regularization coefficient according to the error made at each iteration, with the motivation being that for iterations with large error, large KL regularization weight should be imposed to prevent the agent from going in the wrong update direction. We prove the resulting error propagation bound has the form of *norm-over-weighted-summation* (Theorem 2), which has the potential to more effectively improve the trade-off between learning speed and robustness than uniform averaging.

The rest of the paper is organized as follows. We introduce the notations used and review existing constant KL coefficient RL algorithms in Section 2. In Section 3, we study ADP with a dynamic KL coefficient. Specifically, we discuss our novel design of the KL coefficient, which is based on the maximum iteration-wise error for weighting the effect of regularization. Based on the KL coefficient design, in Section 4 we present a practical RL algorithm, Geometric Value Iteration (GVI). We evaluate GVI on simple mazes and a set of classic control tasks in Section 5. Our experiments show that GVI can converge faster and more stably and that, moreover, GVI with a deep neural network demonstrates significantly stabilized learning compared to constant regularization, even without target networks. Related works and a discussion are given in Section 6. Section 7 presents our conclusions.

2. Background and Notations

We consider a discounted Markov Decision Process (MDP) defined by a tuple $\{\mathcal{S}, \mathcal{A}, P, r, d_0, \gamma\}$, where \mathcal{S} is the finite state space, \mathcal{A} is the finite set of actions, $P \in \Delta_{\mathcal{S} \times \mathcal{A}}^{\mathcal{S}}$ is the transition kernel (writing Δ_X as the probability simplex over the set X , and X^Y is the set of applications from X to Y), $r \in \mathbb{R}^{\mathcal{S} \times \mathcal{A}}$ is the reward function bounded by r_{\max} , $d_0 \in \Delta_{\mathcal{S}}$ is the distribution of the initial state, and $\gamma \in (0, 1)$ is the discount factor. A policy $\pi \in \Delta_{\mathcal{A}}^{\mathcal{S}}$ maps states to a distribution over actions, and we write the expectation over trajectories induced by π and d_0 as \mathbb{E}_{π} , where we omit the notation d_0 for simplicity. For a policy π , the state-action value function is defined as $q_{\pi}(s, a) = \mathbb{E}_{\pi} [\sum_{t=0}^{\infty} \gamma^t r(S_t, A_t) | S_0 = s, A_0 = a]$, and the (un-normalized) discounted visitation frequency is defined as $d_{\pi}(s) = \mathbb{E}_{\pi} [\sum_{t=0}^{\infty} \gamma^t P(S_t = s)]$.

Following [Vieillard et al. \(2020a\)](#), we define a component-wise dot product $\langle f_1, f_2 \rangle = (\sum_a f_1(s, a) f_2(s, a))_s \in \mathbb{R}^{\mathcal{S}}$ for $f_1, f_2 \in \mathbb{R}^{\mathcal{S} \times \mathcal{A}}$, which is useful for expectation calculations. We define $Pv = (\sum_{s'} P(s'|s, a) v(s'))_{s, a} \in \mathbb{R}^{\mathcal{S} \times \mathcal{A}}$ for $v \in \mathbb{R}^{\mathcal{S}}$. We also define a policy-induced transition kernel P_π as $P_\pi q = P\langle \pi, q \rangle$. We write the Bellman evaluation operator $T_\pi q = r + \gamma P_\pi q$ and its unique fixed point as q_π . An optimal policy satisfies $\pi_* \in \operatorname{argmax}_{\pi \in \Delta_{\mathcal{A}}^{\mathcal{S}}} q_\pi$, and $q_* = q_{\pi_*}$. We denote the set of greedy policies w.r.t. $q \in \mathbb{R}^{\mathcal{S} \times \mathcal{A}}$ as $\mathcal{G}(q) = \operatorname{argmax}_{\pi \in \Delta_{\mathcal{A}}^{\mathcal{S}}} \langle q, \pi \rangle$. When scalar functions are applied to vectors, their applications should be understood in a point-wise fashion. KL divergence and Shannon entropy are the two most widely used entropy terms for regularization. We express KL divergence as $\operatorname{KL}(\pi_1 || \pi_2) = \langle \pi_1, \ln \pi_1 - \ln \pi_2 \rangle \in \mathbb{R}^{\mathcal{S}}$ and Shannon entropy (or simply entropy) as $\mathcal{H}(\pi) = \langle -\pi, \ln \pi \rangle \in \mathbb{R}^{\mathcal{S}}$.

Mirror Descent Value Iteration [Vieillard et al. \(2020a\)](#) provides a generalized framework for KL-regularized ADP schemes. The framework, termed Mirror Descent Policy Iteration (MD-PI), is given in Eq. (1), where the equation sign indicates the *component-wise update* of a vector. While MD-PI can also consider the popular Shannon entropy regularization ([Haarnoja et al., 2017](#)), Shannon entropy does not provide an advantage in the theoretical error propagation analysis of MD-PI ([Vieillard et al., 2020a](#)). Accordingly, in this paper, we focus only on the KL regularization.

$$\text{MD-PI} \quad \begin{cases} \pi_{k+1} &= \mathcal{G}_{\pi_k}^\lambda(q_k) \\ q_{k+1} &= (T_{\pi_{k+1} | \pi_k}^\lambda)^m q_k + \epsilon_{k+1} \end{cases}. \quad (1)$$

In Eq. (1), we start from a uniform policy π_0 and evaluate the next policy by applying the greedy operator $\mathcal{G}_\mu^\lambda(q) = \operatorname{argmax}_{\pi \in \Delta_{\mathcal{A}}^{\mathcal{S}}} (\langle \pi, q \rangle - \lambda \operatorname{KL}(\pi || \mu))$ with an arbitrary baseline policy $\mu \in \Delta_{\mathcal{A}}^{\mathcal{S}}$. Usually, μ is chosen as the previous policy. With the obtained regularized greedy policy, we evaluate its action value function q_{k+1} by applying m times the regularized Bellman operator $T_{\pi | \mu}^\lambda q = r + \gamma P (\langle \pi, q \rangle - \lambda_k \operatorname{KL}(\pi || \mu))$. Setting $m = 1, \infty$ corresponds to value iteration and policy iteration schemes, respectively. Setting m to any other value implies the use of approximate modified policy iteration ([Puterman and Shin, 1978](#); [Scherrer et al., 2015](#)). We call Eq. (1) with $m = 1$ the Mirror Descent Value Iteration (MD-VI). The error term ϵ_{k+1} is a vector of the same shape as the action value function, and it is typically assumed that the greedy step is free of error ([Vieillard et al., 2020a](#)).

By the Fenchel conjugacy ([Boyd and Vandenberghe, 2004](#)), the greedy policy π_{k+1} can be analytically obtained as $\mathcal{G}_\mu^\lambda(q) \propto \mu \exp(\frac{q}{\lambda})$ ([Geist et al., 2019](#)). By choosing $\mu = \pi_k$, a direction induction shows that the MD-PI policy π_{k+1} averages all previous Q -values as $\pi_{k+1} \propto \pi_k \exp \frac{q_k}{\lambda} \propto \dots \propto \exp \frac{1}{\lambda} \sum_{j=0}^k q_j$. Since the errors are additive, π_{k+1} also averages errors from previous iterations. Indeed, the following theorem formally shows that the finite-time bound of MD-VI depends on the *norm of the average* of the accumulated errors (the extension to $m > 1$ remaining an open question).

Theorem 1 ([Vieillard et al. \(2020a\)](#)) *Define the maximum value of $\|q_k\|_\infty$ as q_{max} . The ℓ_∞ -bound of MD-VI is*

$$\|q_* - q_{\pi_{k+1}}\|_\infty \leq \frac{2}{(1-\gamma)} \frac{1}{k} \left(\left\| \sum_{j=1}^k \epsilon_j \right\|_\infty + 2q_{max} + \lambda \gamma \ln |\mathcal{A}| \right). \quad (2)$$

In Theorem 1, the optimality gap $\|q_* - q_{\pi_{k+1}}\|_\infty$ is expressed in terms of errors $\frac{1}{k} \sum_{j=1}^k \epsilon_j$, which are averaged with respect to the uniform distribution. This corresponds to having a constant coefficient-KL regularization throughout learning (i.e., fixing λ). Under mild assumptions, such as the sequence of errors having martingale difference under the natural filtration (Azar et al., 2012), the summation of errors asymptotically cancels out. However, the asymptotic cancelation of errors happens only under specific conditions. When the conditions are not satisfied, having a constant coefficient assumes the errors contribute equally (i.e., $\frac{1}{k}$) to the gap $\|q_* - q_{\pi_{k+1}}\|_\infty$, which is often not the case, since in the early stages of learning the errors are typically large and require more attention.

Our motivation comes from the intuition of weighting down large errors using large regularization coefficients λ_k , and thus the weighted average of errors $\frac{1}{\sum_{j=1}^k 1/\lambda_j} \|\sum_{j=1}^k \epsilon_j / \lambda_j\|_\infty$ could be much smaller than that of uniform averaging $\frac{1}{k} \|\sum_{j=1}^k \epsilon_j\|_\infty$. This corresponds to setting a different KL coefficient for each iteration. Intuitively, different coefficients allow for more robust convergence and potentially faster convergence since the magnitude of $\frac{1}{\sum_{j=1}^k 1/\lambda_j} (\epsilon_j / \lambda_j)$ could be much smaller than $\frac{1}{k} \epsilon_j$ if we are allowed to specify the coefficient λ_j . This motivation prompts the use of a *dynamic error-aware* KL coefficient design that is detailed in Section 3.

3. Dynamic Error-Aware KL Regularization

While MD-VI is generally robust against zero-mean errors because the summation of errors asymptotically cancels out, in some situations the errors fail to cancel each other out and result in bad performance of MD-VI. As a concrete example, consider the following errors induced every K step:

$$\begin{cases} \epsilon_k \sim \text{unif}(0, K) & \text{if } k = K, 2K, \dots \\ \epsilon_k = 0 & \text{otherwise} \end{cases}. \quad (3)$$

This artificial example can be likened to a two-state MDP case (Figure 2) where the agent starting from state 1 continues to loop onto itself with zero cost and probability $\frac{K-1}{K}$, and with probability $\frac{1}{K}$ the agent goes to state 2 with cost $\text{unif}(0, K)$ and then back again to state 1.

Figure 1 illustrates the optimality gap of MD-VI under randomly generated 5×5 mazes and errors of Eq. (3) with $K = 100$ (see the environment’s details in Appendix D). In this simple setup, trials with small regularization coefficients (blue line) fail to converge due to performance oscillation brought by the error in Eq. (3), while larger regularization (yellow and green lines) achieves convergence to the optimal policy but at a much slower rate. A suitable strategy in this example is obviously an *error-aware* regularization strategy: being conservative only when the errors are present, and greedy otherwise.

To overcome the limitations of the constant-weight regularization scheme, we study the following regularized PI scheme with a dynamic KL coefficient λ_k :

$$\begin{cases} \pi_{k+1} & = \mathcal{G}_{\pi_k}^{\lambda_k}(q_k) \\ q_{k+1} & = (T_{\pi_{k+1}|\pi_k}^{\lambda_k})^m q_k + \epsilon_{k+1} \end{cases}. \quad (4)$$

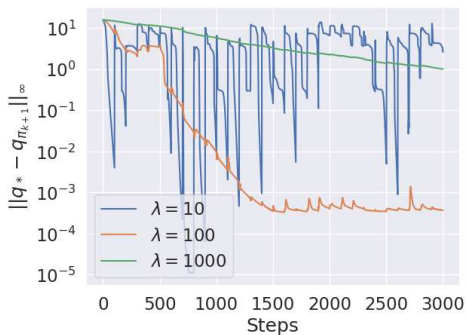


Figure 1: MD-VI in maze under different values of λ with error generated by Eq. (3). In this case, the optimal regularization strategy is time-dependent.

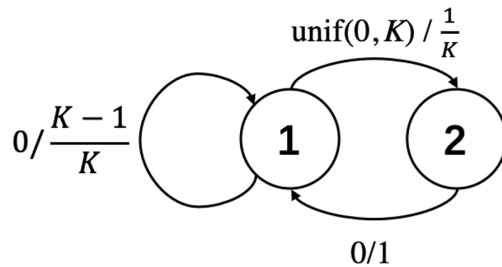


Figure 2: A two-state MDP instantiation of Eq. (3). Numbers on the transitions indicate cost/probability. Such errors might occur in updating weights of neural networks.

We derive the error-aware regularization bound for the policy iteration case. The following theorem provides a bound on the optimality gap of Eq. (4).

Theorem 2 Define $\eta_k = 1/\lambda_k$ and $Z_k = \sum_{j=0}^k \eta_j$. The ℓ_{∞} -bound of Eq. (4) with $m = 1$ is

$$\|q_* - q_{\pi_{k+1}}\|_{\infty} \leq \frac{2}{(1-\gamma)} \frac{1}{Z_k} \left(\left\| \sum_{j=1}^k \eta_j \epsilon_j \right\|_{\infty} + (\eta_{k+1} + \eta_0 + \sum_{j=0}^k |\eta_{j+1} - \eta_j|) q_{max} + \gamma \ln |A| \right). \quad (5)$$

Proof See Appendix A for the proof. ■

Note that this bound generalizes the bound of MD-VI, since Eq. (5) matches Eq. (2) when $\eta = 1/\lambda$. As with MD-VI, this bound features a linear dependency of errors on the horizon $\frac{1}{1-\gamma}$. The main difference is the *weighted average* of the errors instead of the *uniform average* for MD-VI. This weighted average error term intuitively motivates the design of regularization coefficients $\eta_k = 1/\lambda_k$.

First, minimizing the optimality gap implies minimizing $\|\frac{1}{Z_k} \sum_{j=1}^k \eta_j \epsilon_j\|_{\infty}$, which is the norm of the weighted arithmetic mean of errors. Because ϵ_j is a random variable for all j , with $\eta'_j = \frac{\eta_j}{Z_k}$, the mean and the variance of the weighted arithmetic mean are given by $\sum_{j=1}^k \eta'_j \mathbb{E}[\epsilon_j]$ and $\sum_{j=1}^k \eta'_j{}^2 \text{Var}[\epsilon_j]$, respectively. This in turn suggests that η_j should be inversely scaled according to the magnitude of ϵ_j to restrict potentially erroneous updates where errors have huge means or variances. By recalling ϵ_j is a vector, we scale η_j according to the infinity norm as $\eta_j = \frac{1}{\alpha_1 \|\epsilon_j\|_{\infty}}$, where α_1 is used for uniformly scaling all of the coefficients. Note that α_1 does not appear in the error-dependent term since it appears in both numerator η_j and denominator Z_k .

In deep RL, hyperparameters are typically and gradually decayed instead of changed abruptly. This highlights the importance of stability in learning with neural networks, which

we address here. Given the above design choice, we impose an additional constraint that no huge increase from η_k to η_{k+1} is allowed: such an increase during learning can be measured by $\frac{1}{Z_k} \sum_{j=0}^k |\eta_{j+1} - \eta_j|$, which appears in the second term of the error bound Eq. (5). We do not allow the term to diverge by restricting $\eta_{j+1} > 2\eta_j$, which makes $\frac{1}{Z_k} \sum_{j=0}^{k-1} |\eta_{j+1} - \eta_j|$ larger than 1. To this end, we gradually decay the regularization coefficient by introducing another hyperparameter α_2 , such that $\lambda_k = \alpha_2 \lambda_{k-1}$ with $\alpha_2 \in (0, 1)$ generally close to one.

The above-mentioned design choices can be summarized as the following dynamic KL coefficient design:

$$\lambda_k = \max(\alpha_1 \|\epsilon_k\|_\infty, \alpha_2 \lambda_{k-1}), \quad (6)$$

where $\alpha_1 \in \mathbb{R}^+$ and $\alpha_2 \in (0, 1)$.

4. Geometric Value Iteration

In this section we propose a novel algorithm based on the dynamic KL regularization coefficient design of the previous section. While it is straightforward to incorporate it in the general MD-VI scheme of Eq. (4), a crucial subtlety stands in the way of achieving better performance: we know $\pi_{k+1} \propto \exp(\sum_{j=1}^k q_j)$ from Section 2, which requires remembering all previous value functions. In practice, approximation such as information projection would have to be used (Vieillard et al., 2020d), which brings errors to the policy update step.

Leveraging the very recent idea of *implicit KL regularization* (Vieillard et al., 2020c), it is possible to circumvent the need for remembering all previous values in MD-VI by augmenting the reward with a log-policy term, whose formulation is given in Eq. (7). The reward function is augmented by the term $\ln \pi_{k+1}$ weighted by the KL coefficient λ :

$$\begin{cases} \pi_{k+1} = \operatorname{argmax}_{\pi \in \Delta_{\mathcal{A}}^S} \langle \pi, q_k \rangle - \lambda \mathcal{H}(\pi) \\ q_{k+1} = \lambda \ln \pi_{k+1} + r + \gamma P \langle \pi_{k+1}, q_k - \lambda \ln \pi_{k+1} \rangle \end{cases} \quad (7)$$

Eq. (7) corresponds to implicitly performing KL regularization, and hence there is no need for remembering previous values, that is, computing the term $\ln \pi_{k+1}$ suffices.

While Eq. (7) provides an easy-to-use scheme for our dynamic KL coefficient by replacing λ with λ_k , the term $\lambda_k \ln \pi_k$ could cause numerical issues when λ_k has a huge value. For numerical stability, we propose further transforming Eq. (7) as follows:

$$\begin{cases} \pi_{k+1} = \operatorname{argmax}_{\pi \in \Delta_{\mathcal{A}}^S} \langle \pi, q_k \rangle + \mathcal{H}(\pi) \\ q_{k+1} = \ln \pi_{k+1} + \frac{r}{\lambda_{k+1}} + \frac{\lambda_k}{\lambda_{k+1}} \gamma P \langle \pi_{k+1}, q_k - \ln \pi_{k+1} \rangle \end{cases} \quad (8)$$

Additional clipping might also be necessary to restrict the magnitude of $\ln \pi_{k+1}$. We can show that the scheme of Eq. (8) is equivalent to the formulation of Eq. (4), which we formally state below.

Theorem 3 *For any $k \geq 0$, by defining $q'_k = \lambda_{k+1} (q_k - \ln \pi_k)$, we have*

$$(8) \Leftrightarrow \begin{cases} \pi_{k+1} = \operatorname{argmax}_{\pi \in \Delta_{\mathcal{A}}^S} \langle \pi, q'_k \rangle - \lambda_k \operatorname{KL}(\pi \| \pi_k) \\ q'_{k+1} = r + \gamma P \langle \pi_{k+1}, q'_k - \lambda_k \operatorname{KL}(\pi_{k+1} \| \pi_k) \rangle \end{cases} \quad (9)$$

Proof See Appendix B for the proof. ■

By dynamically adjusting the KL coefficient, Eq. (8) mitigates issues brought by various sources of error and improves learning stability. One more problem remains for making Eq. (8) practically applicable. In tuning the KL coefficient Eq. (6), the magnitude information of $\|\epsilon_{k+1}\|_\infty$ is typically unavailable. Taking inspiration from a very recent work (Vieillard et al., 2020b), we approximately compute this error by moving average TD-error from batches. Hence, we approximate $\|\epsilon_{k+1}\|_\infty$ by the maximum absolute TD error $\|\epsilon_{\text{TD},i}\|_\infty$, where i indicates the i th batch. In summary, our Geometric Value Iteration (GVI) iterates as follows:

$$\text{GVI} \begin{cases} \lambda_{k+1} = \max(\alpha_1 \|\epsilon_{\text{TD},k}\|_\infty, \alpha_2 \lambda_k) \\ \pi_{k+1} = \operatorname{argmax}_{\pi \in \Delta^{\mathcal{A}}} \langle \pi, q_k \rangle + \mathcal{H}(\pi) \\ q_{k+1} = \ln \pi_{k+1} + \frac{r}{\lambda_{k+1}} + \frac{\lambda_k}{\lambda_{k+1}} \gamma P \langle \pi_{k+1}, q_k - \ln \pi_{k+1} \rangle \end{cases}. \quad (10)$$

The name *Geometric* comes from the fact that GVI mixes two policies by weighted *geometric* mean as $\pi_{k+1} = \mathcal{G}_{\pi_k}^{\lambda_k}(q_k) \propto (\pi_k)^{1-\zeta_k} (\mathcal{G}_{\pi_k}^\lambda(q_k))^{\zeta_k}$, where $\lambda/\zeta_k = \lambda_k$.

We now present the implementation of Eq. (10) using deep networks, or Deep GVI (DGVI). Suppose Q -values are estimated by an online Q network parameterized by weight vector θ and the transition data are stored in a FIFO replay buffer \mathcal{B} . DGVI minimizes the following loss function:

$$L_\theta = \mathbb{E}_{(s,a,r,s') \sim \mathcal{B}} \left[(q_\theta(s,a) - y(s,a))^2 \right], \quad (11)$$

$$\text{where } y(s,a) = \ln \pi(a|s) + \frac{r(s,a)}{\lambda'} + \frac{\lambda}{\lambda'} \gamma \mathbb{E}_{a' \sim \pi(\cdot|s')} [q_{\bar{\theta}}(s',a') - \ln \pi(a'|s')], \quad (12)$$

where $\bar{\theta}$ indicates the weight vector of the target network and $\pi \propto \exp(q_{\bar{\theta}})$ is the greedy policy. λ and λ' are the previous and current KL coefficients, respectively. The use of slowly updated target network $q_{\bar{\theta}}$ in the target $y(s,a)$ is conventional for stability purposes. The parameters $\bar{\theta}$ are either infrequently copied from θ or obtained by Polyak averaging $\bar{\theta}$. While target networks could be used to further enhance the performance, in our experiments we explicitly remove target networks to highlight the error-robustness of DGVI.

Taking inspiration from (Vieillard et al., 2020b), we use the moving average of maximum batch TD errors to approximate the maximum error based on Eq. (8):

$$\begin{aligned} \lambda' &\leftarrow (1 - \nu)\lambda' + \nu \max(\alpha_1 \|\epsilon_{\text{TD}}\|_\infty, \alpha_2 \lambda) \\ \lambda &\leftarrow (1 - \nu_{\text{slow}})\lambda + \nu_{\text{slow}}\lambda' \end{aligned}, \quad (13)$$

where $\|\epsilon_{\text{TD}}\|_\infty$ is the maximum absolute TD error in a batch, and ν and ν_{slow} are learning rates for λ and λ' , respectively. We summarize the algorithm of DGVI in Algorithm. 1.

5. Experiments

This section empirically studies the proposed GVI with tabular and deep implementation. We wanted to evaluate the effectiveness of our error-aware KL coefficient design in handling the trade-off between learning speed and stability. For didactic purposes, we first evaluated

Algorithm 1 Deep Geometric Value Iteration

- 1: Initialize θ , λ and λ'
 - 2: **for** each iteration **do**
 - 3: Collect transitions and add them to \mathcal{B}
 - 4: **for** each gradient step **do**
 - 5: Compute the maximum absolute TD error $\|\epsilon_{\text{TD}}\|_{\infty}$ in a minibatch.
 - 6: Update λ and λ' using Eq. (13).
 - 7: Update θ with one step of SGD using Eq. (11)
 - 8: **end for**
 - 9: **end for**
-

GVI on a tabular maze environment that is the same as the one used in Figure 1. The tabular experiments serve to verify that GVI can better handle the trade-off problem between learning speed and robustness than the constant KL coefficient scheme. We then conducted an experiment on classic control tasks from OpenAI Gym benchmarks (Brockman et al., 2016) to observe the behavior of GVI with deep implementation. For the deep RL experimentation, we consider GVI as a variation of Munchausen-DQN (M-DQN) (Vieillard et al., 2020c) and thus take M-DQN as our baseline.

Tabular Experiments Figure 3 investigates the optimality gap of GVI with varying conditions. For GVI, we also included the investigation of the introduced hyperparameters α_1 and α_2 and their impact on performance. Although they do not play any role in error analysis, in practice they can have a large effect on the trade-off between speed and stability.

The left graph in Figure 3 compares the best behavior of GVI with MD-VI, where the parameters of GVI are fine-tuned to yield the empirically best performance. The figure shows that GVI achieves faster and more robust convergence than MD-VI under a certain hyperparameter. GVI reaches the minimum optimality gap in around 50 steps and keeps the value under 10^{-3} . On the other hand, MD-VI suffers from the trade-off between speed and stability. While $\lambda = 50$ reaches the minimum optimality gap close to that of GVI, it reaches it in around 1000 steps and is thus much slower than GVI. MD-VI with $\lambda = 30$ converges faster, but the optimality gap oscillates and exceeds 10^{-2} . Therefore, it can be safely concluded that the constant KL coefficient scheme MD-VI cannot outperform GVI.

The middle and the right graphs are plotted to investigate the behavior of GVI with different α_1 and α_2 . GVI with a small α_1 never reaches the optimal value, while experiments with the small α_2 obtain a small optimality gap at the cost of huge oscillation. These are expected since λ_k corresponds to the learning rate of the updates (Kozuno et al., 2019), and α_2 decides how long the conservativeness remains after detecting large errors.

Deep RL Experiments Using a set of classic control benchmarks (Brockman et al., 2016), we examine the DGVI of Algorithm. 1 against the constant KL coefficient algorithm of M-DQN (Vieillard et al., 2020c). We choose the LunarLander-v2, CartPole-v1, and Pendulum-v0 environments as our benchmarks. Since our DGVI and M-DQN support only discrete action space environments, we discretized the continuous action space of Pendulum-v0 into five discrete actions. For each seed we perform 10 evaluation roll-outs every 300 environment steps. For a fair comparison, all of the algorithms share the

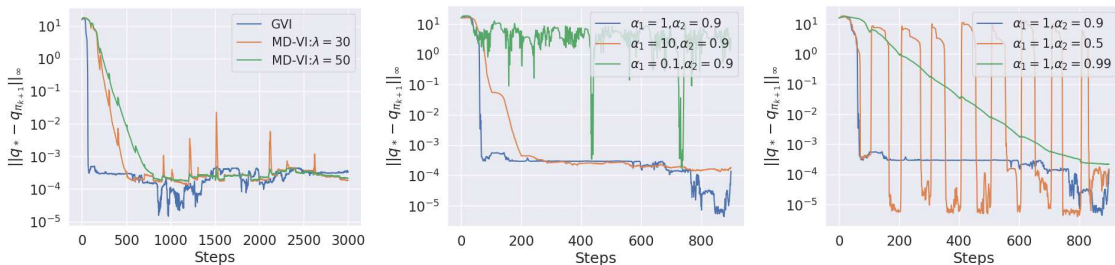


Figure 3: (Left) Performance comparison of GVI ($\alpha_1 = 2, \alpha_2 = 0.9$) and MD-PI($\lambda = 30, \lambda = 50$). (Middle) GVI with different α_1 . (Right) GVI with different α_2 .

same hyperparameters except the KL regularization. To highlight the robustness of algorithms against estimation errors, we explicitly remove target networks from the algorithms, even though such networks provide a key ingredient to the success of modern deep RL (Mnih et al., 2015; Haarnoja et al., 2018). All figures are plotted by averaging results from five independent random seeds for statistical results. We list the set of hyperparameters in Appendix C.

Figure 4 shows the learning curves of algorithms and the corresponding KL regularization of DGVI. Compared to the constant regularized algorithms, GVI achieves more stable learning in DiscretePendulum and CartPole. Notably, GVI has smaller regularization in DiscretePendulum and CartPole than $\lambda = 10$. This indicates that the dynamic change of the KL coefficient is more important than its magnitude.

To observe how the dynamic KL coefficient improves stability, we evaluated the maximum absolute TD error $\|\epsilon_{\text{TD}}\|_\infty$ as shown in Figure 5. Compared to constant regularized algorithms, the error of DGVI proves to be much smaller during learning. This result agrees well with how DGVI updates the network by Eq. (11): the bootstrap is scaled by $\frac{\lambda'}{\lambda}$, which becomes small when DGVI encounters large errors. For a better understanding of the effect on the bootstrap, consider an extreme case where a significantly huge error is induced and λ' is infinite. Then, the loss becomes $L_\theta \approx \mathbb{E}_{(s,a) \sim \mathcal{B}} \left[(q_\theta(s,a) - \ln \pi(s,a))^2 \right] = \mathbb{E}_{s \sim \mathcal{B}} \left[\left(\ln \sum_{a \in \mathcal{A}} \exp(q_\theta(s,a)) \right)^2 \right]$, and thus the new q_θ will have smaller values. GVI thus tends to underestimate the state and action pairs where huge errors are expected, which is assumed to prevent bad updates from quickly spreading to downstream Q -values. We can conclude that the proposed mechanism renders DGVI stable even without target networks.

6. Related Work and Discussion

The recent boom in the literature on KL-regularized ADP (Azar et al., 2012; Ghavamzadeh et al., 2011; Bellemare et al., 2016; Vieillard et al., 2020d; Kozuno et al., 2019) has demonstrated the effectiveness of KL regularization against estimation errors. The most relevant algorithms to our proposed approach are Mirror Descent Value Iteration (MD-VI) (Geist et al., 2019) and Munchausen Value Iteration (MVI) (Vieillard et al., 2020c); those algorithms introduce a KL penalty on both the greedy and the evaluation steps. While some studies have focused on the error bounds of KL-regularized AVI (Vieillard et al., 2020a), how dynamic

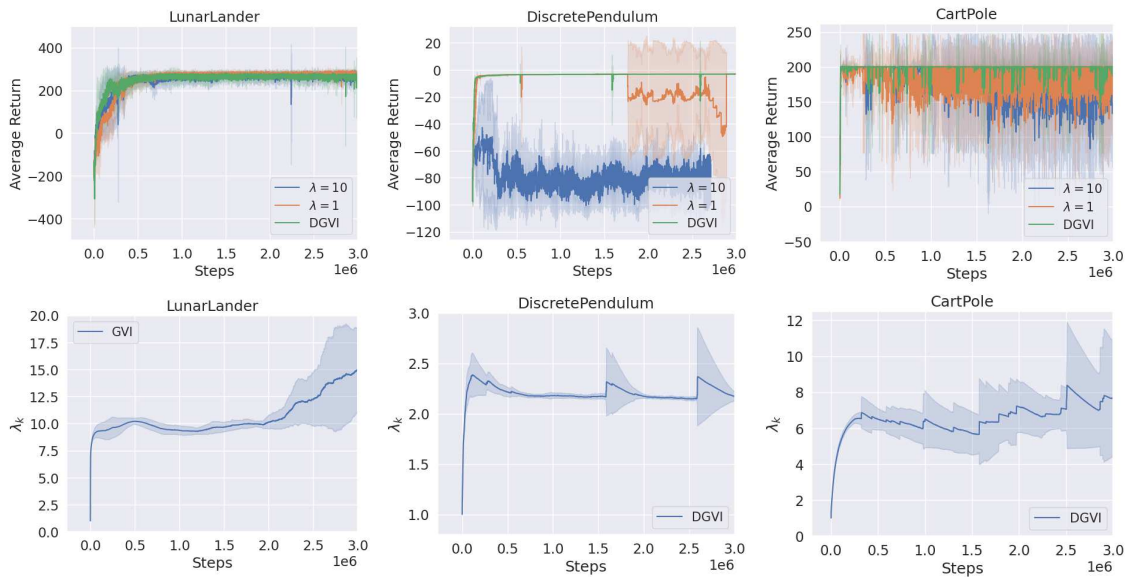


Figure 4: (Top) Training curves on the discrete control tasks and (bottom) the KL coefficient in DGVI. The solid curves show the mean and the shaded regions show the standard deviation over the five independent trials.

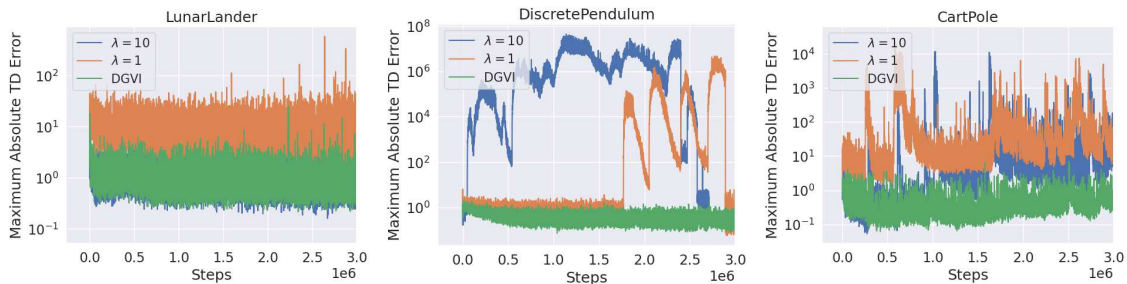


Figure 5: The maximum absolute TD errors. The results are averaged over the five independent trials. DGVI shows much smaller TD errors in DiscretePendulum and CartPole.

changes in the regularization coefficient affect performance has been left largely untouched. To the best of our knowledge, this paper is the first work to provide the error bound of an AVI with dynamic KL regularization.

While it has not been discussed in the ADP literature, dynamic KL regularization has appeared in many deep RL algorithms. Dynamic KL regularization is often introduced to restrict aggressive policy improvement steps. Trust region policy optimization (TRPO) (Schulman et al., 2015) is one such seminal algorithm that introduces KL constraints to approximately ensure monotonic improvement. Based on TRPO, many algorithms leverage the KL constraint and demonstrate promising performance on challenging environments (Schulman et al., 2017; Nachum et al., 2018; Abdolmaleki et al., 2018), and

Nachum et al. (2018) introduced a dynamic KL coefficient design to create a trust region. However, the above-mentioned algorithms design the dynamic coefficient based on heuristics, while we design it by leveraging rigorous analysis as shown in Theorem 2. Furthermore, trust-region methods consider the KL constraints even when there are no estimation errors, and thus they may overly slow down learning.

In addition to the dynamic KL regularization, DGVI has an important feature: error awareness. One of the most well-known algorithms making use of TD error is Prioritized Experience Replay (PER) (Schaul et al., 2015). PER utilizes TD error for prioritizing the samples in the replay buffer to increase the appearance of rare samples. On the other hand, DGVI mitigates the effect of rare samples that may have huge TD errors by scaling its bootstrapping. Thus, slower learning will be expected when exploration matters: the rare samples will have less of an affect than usual in DGVI. We do not consider this problem as exploration that is out of our scope.

In this work, we do not consider Shannon entropy for regularization. Some entropy regularized ADP literature has established that by augmenting the reward with Shannon entropy, the optimal policy becomes multi-modal and hence robust against adversarial settings (Haarnoja et al., 2017, 2018; Ahmed et al., 2019). We leave GVI with Shannon entropy regularization as future work due to the complex theoretical analysis.

7. Conclusion

We have presented the first *error-aware* KL coefficient design for RL algorithms and developed a novel *error-aware* RL algorithm, Geometric Value Iteration (GVI), which features a dynamic *error-aware* KL coefficient design aimed at mitigating the impact of errors on performance. The theoretical error bound analysis provides two guidelines for efficient learning: The coefficient should be increased when a large error is induced but its effect should not be overly large. This dynamic regularization allows GVI to address the trade-off problem between robustness and convergence speed, which has been largely left untouched in previous ADP studies.

In addition to GVI as an ADP scheme, we further combined GVI with deep networks. Based on the recent framework introduced by Vieillard et al. (2020c), we implement GVI as a deep RL algorithm, and the resulting algorithm, deep GVI (DGVI), achieves robustness against errors by reducing the bootstrapping effect when it meets huge TD errors. Our experiments verified not only the faster and more stable learning of GVI but also the more robust learning of DGVI even without target networks.

While our algorithm can be easily applied to standard deep RL frameworks, our empirical studies are limited to classic control tasks due to the expensive computational cost of recent Deep RL benchmarks, e.g., Atari games (Bellemare et al., 2013). We believe that the classic control tasks are sufficient to verify our algorithms and thus leave evaluation on a set of high-dimensional benchmarks as future work.

Acknowledgments

This work is partly supported by JSPS KAKENHI Grant Number 21H03522 and 21J15633.

References

- Abbas Abdolmaleki, Jost Tobias Springenberg, Yuval Tassa, Remi Munos, Nicolas Heess, and Martin Riedmiller. Maximum a posteriori policy optimisation. In *International Conference on Learning Representations*, pages 1–22, 2018.
- Zafarali Ahmed, Nicolas Le Roux, Mohammad Norouzi, and Dale Schuurmans. Understanding the impact of entropy on policy optimization. In *International Conference on Machine Learning*, pages 151–160, 2019.
- Mohammad Gheshlaghi Azar, Vicenç Gómez, and Hilbert J Kappen. Dynamic policy programming. *The Journal of Machine Learning Research*, 13(1):3207–3245, 2012.
- Marc G Bellemare, Yavar Naddaf, Joel Veness, and Michael Bowling. The arcade learning environment: An evaluation platform for general agents. *Journal of Artificial Intelligence Research*, 47:253–279, 2013.
- Marc G Bellemare, Georg Ostrovski, Arthur Guez, Philip Thomas, and Rémi Munos. Increasing the action gap: New operators for reinforcement learning. In *AAAI Conference on Artificial Intelligence*, pages 1476–1483, 2016.
- Dimitri P Bertsekas and John N Tsitsiklis. *Neuro-dynamic programming*. Athena Scientific, 1996.
- Stephen Boyd and Lieven Vandenberghe. *Convex Optimization*. Cambridge University Press, USA, 2004.
- Greg Brockman, Vicki Cheung, Ludwig Pettersson, Jonas Schneider, John Schulman, Jie Tang, and Wojciech Zaremba. OpenAI Gym. *arXiv preprint arXiv:1606.01540*, 2016.
- Justin Fu, Aviral Kumar, Matthew Soh, and Sergey Levine. Diagnosing bottlenecks in deep Q-learning algorithms. In *International Conference on Machine Learning*, pages 2021–2030, 2019.
- Scott Fujimoto, Herke Hoof, and David Meger. Addressing function approximation error in actor-critic methods. In *International Conference on Machine Learning*, pages 1587–1596, 2018.
- Matthieu Geist, Bruno Scherrer, and Olivier Pietquin. A theory of regularized Markov decision processes. In *International Conference on Machine Learning*, pages 2160–2169, 2019.
- Mohammad Ghavamzadeh, Hilbert Kappen, Mohammad Azar, and Rémi Munos. Speedy Q-learning. *Advances in Neural Information Processing Systems*, 24:2411–2419, 2011.
- Tuomas Haarnoja, Haoran Tang, Pieter Abbeel, and Sergey Levine. Reinforcement learning with deep energy-based policies. In *International Conference on Machine Learning*, pages 1352–1361, 2017.

- Tuomas Haarnoja, Aurick Zhou, Pieter Abbeel, and Sergey Levine. Soft actor-critic: Off-policy maximum entropy deep reinforcement learning with a stochastic actor. In *International Conference on Machine Learning*, pages 1861–1870, 2018.
- Sham Kakade and John Langford. Approximately optimal approximate reinforcement learning. In *International Conference on Machine Learning*, page 267–274, 2002.
- Tadashi Kozuno, Eiji Uchibe, and Kenji Doya. Theoretical analysis of efficiency and robustness of softmax and gap-increasing operators in reinforcement learning. In *Artificial Intelligence and Statistics Conference*, pages 2995–3003, 2019.
- Timothy P Lillicrap, Jonathan J Hunt, Alexander Pritzel, Nicolas Heess, Tom Erez, Yuval Tassa, David Silver, and Daan Wierstra. Continuous control with deep reinforcement learning. In *International Conference on Learning Representations*, pages 1–14, 2015.
- Volodymyr Mnih, Koray Kavukcuoglu, David Silver, Andrei A Rusu, Joel Veness, Marc G Bellemare, Alex Graves, Martin Riedmiller, Andreas K Fidjeland, Georg Ostrovski, et al. Human-level control through deep reinforcement learning. *Nature*, 518(7540):529–533, 2015.
- Rémi Munos and Csaba Szepesvári. Finite-time bounds for fitted value iteration. *Journal of Machine Learning Research*, 9(27):815–857, 2008.
- Ofir Nachum, Mohammad Norouzi, Kelvin Xu, and Dale Schuurmans. Trust-PCL: An off-policy trust region method for continuous control. In *International Conference on Learning Representations*, pages 1–14, 2018.
- Martin L Puterman and Moon Chirl Shin. Modified policy iteration algorithms for discounted Markov decision problems. *Management Science*, 24(11):1127–1137, 1978.
- Tom Schaul, John Quan, Ioannis Antonoglou, and David Silver. Prioritized experience replay. In *International Conference on Learning Representations*, pages 1–21, 2015.
- Bruno Scherrer, Mohammad Ghavamzadeh, Victor Gabillon, Boris Lesner, and Matthieu Geist. Approximate modified policy iteration and its application to the game of tetris. *Journal of Machine Learning Research*, 16:1629–1676, 2015.
- John Schulman, Sergey Levine, Pieter Abbeel, Michael Jordan, and Philipp Moritz. Trust region policy optimization. In *International Conference on Machine Learning*, pages 1889–1897, 2015.
- John Schulman, Filip Wolski, Prafulla Dhariwal, Alec Radford, and Oleg Klimov. Proximal policy optimization algorithms. *arXiv preprint arXiv:1707.06347*, 2017.
- David Silver, Julian Schrittwieser, Karen Simonyan, Ioannis Antonoglou, Aja Huang, Arthur Guez, Thomas Hubert, Lucas Baker, Matthew Lai, Adrian Bolton, et al. Mastering the game of go without human knowledge. *Nature*, 550(7676):354–359, 2017.

- Nino Vieillard, Tadashi Kozuno, Bruno Scherrer, Olivier Pietquin, Rémi Munos, and Matthieu Geist. Leverage the average: an analysis of KL regularization in reinforcement learning. In *Advances in Neural Information Processing Systems*, pages 12163–12174, 2020a.
- Nino Vieillard, Olivier Pietquin, and Matthieu Geist. Deep conservative policy iteration. In *AAAI Conference on Artificial Intelligence*, pages 6070–6077, 2020b.
- Nino Vieillard, Olivier Pietquin, and Matthieu Geist. Munchausen reinforcement learning. In *Advances in Neural Information Processing Systems*, pages 4235–4246, 2020c.
- Nino Vieillard, Bruno Scherrer, Olivier Pietquin, and Matthieu Geist. Momentum in reinforcement learning. In *International Conference on Artificial Intelligence and Statistics*, pages 2529–2538, 2020d.

Appendix A. Proofs on the performance bound

For the following proof, we define the greedy policy and the Bellman operator regularized by Shannon entropy as well as KL divergence as $\mathcal{G}_\mu^{\lambda, \tau}(q) = \operatorname{argmax}_{\pi \in \Delta_{\mathcal{A}}^S} (\langle \pi, q \rangle - \lambda \operatorname{KL}(\pi || \mu) + \tau \mathcal{H}(\pi))$ and $T_{\pi || \mu}^{\lambda, \tau} q = r + \gamma P (\langle \pi, q \rangle - \lambda \operatorname{KL}(\pi || \mu)) + \tau \mathcal{H}(\pi)$, respectively. We also note the following fact about the greedy policy (Vieillard et al., 2020a):

$$\mathcal{G}_\mu^{\lambda, \tau}(q) = \operatorname{argmax}_{\pi \in \Delta_{\mathcal{A}}^S} (\langle \pi, q \rangle - \lambda \operatorname{KL}(\pi || \mu) + \tau \mathcal{H}(\pi)) \propto \mu^{\frac{\lambda}{\lambda + \tau}} \exp \frac{1}{\lambda + \tau} q, \quad (14)$$

and we have the following maximum:

$$\max_{\pi \in \Delta_{\mathcal{A}}^S} (\langle \pi, q \rangle - \lambda \operatorname{KL}(\pi || \mu) + \tau \mathcal{H}(\pi)) = (\lambda + \tau) \ln \langle \mathbf{1}, \mu^{\frac{\lambda}{\lambda + \tau}} \exp \frac{q}{\lambda + \tau} \rangle. \quad (15)$$

Before going to the proof of Theorem 2, we provide the following proposition.

Proposition 4 Define $Z_k = \sum_{j=0}^k \eta_j$, $h_0 = q_0$, and h_k for $k \geq 1$ as the average of past smoothed q -functions: $h_k = \frac{1}{Z_k} \sum_{j=0}^k \eta_j q_j = \frac{Z_{k-1}}{Z_k} h_{k-1} + \frac{\eta_k}{Z_k} q_k$. If $\lambda_k > 0$ for all k , GVI is equivalent to the following iteration:

$$\begin{cases} \pi_{k+1} = \mathcal{G}^{0, \frac{1}{Z_k}}(h_k) \\ q_{k+1} = (T_{\pi_{k+1} || \pi_k}^{\frac{1}{Z_k}, 0})^m q_k + \epsilon_{k+1} \\ h_{k+1} = \frac{1}{Z_{k+1}} \sum_{j=0}^{k+1} \eta_j q_j = \frac{Z_k}{Z_{k+1}} h_k + \frac{\eta_{k+1}}{Z_{k+1}} q_{k+1}. \end{cases} \quad (16)$$

Proof Using Eq. (14) and by direct induction, we have $\pi_{k+1} \propto \pi_k \exp \eta_k q_k \propto \dots \propto \exp \sum_{j=0}^k \eta_j q_j = \exp Z_k h_k$. Eq. (14) also provides $\operatorname{argmax}_{\pi \in \Delta_{\mathcal{A}}^S} (\langle \pi, q \rangle + \tau \mathcal{H}(\pi)) \propto \exp(\frac{1}{\tau} q)$. Hence, π_{k+1} satisfies $\pi_{k+1} = \operatorname{argmax}_{\pi \in \Delta_{\mathcal{A}}^S} (\langle \pi, h_k \rangle + \frac{1}{Z_k} \mathcal{H}(\pi)) = \mathcal{G}^{0, \frac{1}{Z_k}}(h_k)$. ■

We now prove the error-bound of GVI using Eq. (16).

Proof. We first transform $q_* - q_{\pi_{k+1}}$, the difference between the optimal value function and the value function computed by Eq. (16), using the following useful lemma:

Lemma 5 (Kakade and Langford (2002)) For any $q \in \mathbb{R}^{\mathcal{S} \times \mathcal{A}}$ and $\pi \in \Delta_{\mathcal{A}}^S$, we have $q_\pi - q = (I - \gamma P_\pi)^{-1} (T_\pi q - q)$.

Using Lemma 5, $q_* - q_{\pi_{k+1}}$ can be transformed as

$$\begin{aligned} q_* - q_{\pi_{k+1}} &= q_* - h_k + h_k - q_{\pi_{k+1}} \\ &= (I - \gamma P_{\pi_*})^{-1} (T_{\pi_*} h_k - h_k) - (I - \gamma P_{\pi_{k+1}})^{-1} (T_{\pi_{k+1}} h_k - h_k). \end{aligned} \quad (17)$$

Since the KL regularization vanishes after the iteration converges, the optimal policy must be deterministic, and hence $\mathcal{H}(\pi_*) = 0$. Since π_{k+1} is the regularized greedy policy, we have

$$\begin{aligned} \pi_{k+1} = \mathcal{G}^{0, \frac{1}{Z_k}}(h_k) &\Rightarrow \langle \pi_{k+1}, h_k \rangle + \frac{1}{Z_k} \mathcal{H}(\pi_{k+1}) \geq \langle \pi_*, h_k \rangle + \frac{1}{Z_k} \mathcal{H}(\pi_*) \\ &\Rightarrow T_{\pi_{k+1}}^{0, \frac{1}{Z_k}} h_k = T_{\pi_{k+1}} h_k + \gamma \frac{1}{Z_k} P \mathcal{H}(\pi_{k+1}) \geq T_{\pi_*} h_k. \end{aligned} \quad (18)$$

Using this with Eq. (5) and the fact that for any π the matrix $(I - \gamma P_\pi)^{-1} = \sum_{t \geq 0} \gamma^t P_\pi^t$ is positive, we have the following inequality:

$$q_* - q_{\pi_{k+1}} \leq (I - \gamma P_{\pi_*})^{-1} (T_{\pi_{k+1}}^{0, \frac{1}{Z_k}} h_k - h_k) - (I - \gamma P_{\pi_{k+1}})^{-1} (T_{\pi_{k+1}}^{0, \frac{1}{Z_k}} h_k - h_k - \gamma \frac{1}{Z_k} P \mathcal{H}(\pi_{k+1})). \quad (19)$$

As for the residual $T_{\pi_{k+1}}^{0, \frac{1}{Z_k}} h_k - h_k$, we have the following useful lemma:

Lemma 6 *For any $k \geq 1$, we have $\eta_k T_{\pi_{k+1} | \pi_k}^{\frac{1}{Z_k}, 0} q_k = Z_k T_{\pi_{k+1}}^{0, \frac{1}{Z_k}} h_k - Z_{k-1} T_{\pi_k}^{0, \frac{1}{Z_{k-1}}} h_{k-1}$. For $k = 0$, we have $\eta_0 T_{\pi_1 | \pi_0}^{\frac{1}{Z_0}, 0} q_0 = Z_0 T_{\pi_1}^{0, \frac{1}{Z_0}} h_0 - \gamma P \mathcal{H}(\pi_0)$.*

Proof Using the definition of π_k and h_k , the following equation holds.

$$\eta_k q_k + \ln \pi_k = \eta_k q_k + (Z_{k-1} h_{k-1} - \ln \langle \mathbf{1}, \exp Z_{k-1} h_{k-1} \rangle) = Z_k h_k - \ln \langle \mathbf{1}, \exp Z_{k-1} h_{k-1} \rangle. \quad (20)$$

Therefore, we have $\langle \pi, \eta_k q_k \rangle - \text{KL}(\pi | \pi_k) = \langle \pi, Z_k h_k \rangle - \langle \pi, \ln \pi \rangle - \ln \langle \mathbf{1}, \exp Z_{k-1} h_{k-1} \rangle$. From Eq. (15), the maximum of $\langle \pi, Z_k h_k \rangle - \langle \pi, \ln \pi \rangle$ is $\ln \langle \mathbf{1}, \exp Z_k h_k \rangle$, and the maximizer is π_{k+1} from the definition. By substituting π_{k+1} to π , the following equation holds:

$$\langle \pi_{k+1}, \eta_k q_k \rangle - \text{KL}(\pi_{k+1} | \pi_k) = Z_k \frac{1}{Z_k} \ln \langle \mathbf{1}, \exp Z_k h_k \rangle - Z_{k-1} \frac{1}{Z_{k-1}} \ln \langle \mathbf{1}, \exp Z_{k-1} h_{k-1} \rangle. \quad (21)$$

From Eq. (15), $\frac{1}{Z_k} \ln \langle \mathbf{1}, \exp Z_k h_k \rangle$ is the maximum of $\langle \pi, h_k \rangle + \frac{1}{Z_k} \mathcal{H}(\pi)$, and the associated maximizer is again π_{k+1} . Hence, the following equation holds:

$$\langle \pi_{k+1}, \eta_k q_k \rangle - \text{KL}(\pi_{k+1} | \pi_k) = Z_k \left(\langle \pi_{k+1}, h_k \rangle + \frac{1}{Z_k} \mathcal{H}(\pi_{k+1}) \right) - Z_{k-1} \left(\langle \pi_k, h_{k-1} \rangle + \frac{1}{Z_{k-1}} \mathcal{H}(\pi_k) \right). \quad (22)$$

Observing that $\eta_k r = Z_k r - Z_{k-1} r$, we have the first part of the result: $\eta_k T_{\pi_{k+1} | \pi_k}^{\frac{1}{Z_k}, 0} q_k = Z_k T_{\pi_{k+1}}^{0, \frac{1}{Z_k}} h_k - Z_{k-1} T_{\pi_k}^{0, \frac{1}{Z_{k-1}}} h_{k-1}$. For $k = 0$, using the fact that $h_0 = q_0$,

$$\eta_0 T_{\pi_1 | \pi_0}^{\frac{1}{Z_0}, 0} q_0 = \eta_0 r + \gamma P (\langle \pi_1, \eta_0 h_0 \rangle) + \eta_0 \frac{1}{\eta_0} \mathcal{H}(\pi_1) + \eta_0 \frac{1}{\eta_0} \langle \pi_1, \ln \pi_0 \rangle = \eta_0 T_{\pi_1}^{0, \frac{1}{Z_0}} h_0 - \gamma P \mathcal{H}(\pi_0), \quad (23)$$

where we use in the last line the fact that π_0 , being uniform, $\langle \pi_1, \ln \pi_0 \rangle = -\ln |\mathcal{A}| = -\mathcal{H}(\pi_0)$. This concludes the proof. \blacksquare

Using Lemma 6, we can provide induction on h_k .

Lemma 7 *Define $E_k = -\sum_{j=1}^k \eta_j \epsilon_j$ and $X_k = \sum_{j=0}^k (\eta_{j+1} - \eta_j) T_{\pi_{j+1} | \pi_j}^{\frac{1}{Z_j}, 0} q_j$. For any $k \geq 1$, we have $h_{k+1} = \frac{Z_k}{Z_{k+1}} T_{\pi_{k+1}}^{0, \frac{1}{Z_k}} h_k + \frac{1}{Z_{k+1}} (\eta_0 q_0 - E_{k+1} + X_k - \gamma P \mathcal{H}(\pi_0))$.*

Proof Using the definition of h_k , Lemma 6, and the fact that $q_{k+1} = T_{\pi_{k+1}|\pi_k}^{\frac{1}{Z_k},0} q_k + \epsilon_{k+1}$, we have

$$\begin{aligned}
 Z_{k+1}h_{k+1} &= \sum_{j=0}^{k+1} \eta_j q_j = \eta_0 q_0 + \eta_1 q_1 + \sum_{j=1}^k \eta_{j+1} q_{j+1} \\
 &= \eta_0 q_0 + ((\eta_1 - \eta_0) + \eta_0) T_{\pi_1|\pi_0}^{\frac{1}{Z_0},0} q_0 + \eta_1 \epsilon_1 + \sum_{j=1}^k \left(((\eta_{j+1} - \eta_j) + \eta_j) T_{\pi_{j+1}}^{\frac{1}{Z_j},0} q_j + \eta_{j+1} \epsilon_{j+1} \right) \\
 &= \eta_0 q_0 + \left(Z_0 T_{\pi_1}^{0,\frac{1}{Z_0}} h_0 - \gamma P\mathcal{H}(\pi_0) \right) + \sum_{j=1}^k \left(Z_j T_{\pi_{j+1}}^{0,\frac{1}{Z_j}} h_j - Z_{j-1} T_{\pi_j}^{0,\frac{1}{Z_{j-1}}} h_{j-1} \right) + X_k - E_{k+1} \\
 &= \eta_0 q_0 + X_k - E_{k+1} - \gamma P\mathcal{H}(\pi_0) + Z_k T_{\pi_{k+1}}^{0,\frac{1}{Z_k}} h_k \tag{24}
 \end{aligned}$$

$$\Leftrightarrow h_{k+1} = \frac{Z_k}{Z_{k+1}} T_{\pi_{k+1}}^{0,\frac{1}{Z_k}} h_k + \frac{1}{Z_{k+1}} (\eta_0 q_0 - E_{k+1} + X_k - \gamma P\mathcal{H}(\pi_0)). \tag{25}$$

■

Using Lemma 7 and the fact that $Z_{k+1}h_{k+1} = Z_k h_k + \eta_{k+1} q_{k+1}$, we have $T_{\pi_{k+1}}^{0,\frac{1}{Z_k}} h_k - h_k = \frac{1}{Z_k} (\eta_{k+1} q_{k+1} - \eta_0 q_0 + E_{k+1} - X_k + \gamma P\mathcal{H}(\pi_0))$. Injecting this last result into decomposition (19), we get

$$\begin{aligned}
 q_* - q_{\pi_{k+1}} &\leq (I - \gamma P_{\pi_*})^{-1} (T_{\pi_{k+1}}^{0,\frac{1}{Z_k}} h_k - h_k) - (I - \gamma P_{\pi_{k+1}})^{-1} (T_{\pi_{k+1}}^{0,\frac{1}{Z_k}} h_k - h_k - \gamma P\mathcal{H}(\pi_{k+1})) \\
 &\leq (I - \gamma P_{\pi_*})^{-1} \left(\frac{1}{Z_k} (Y_k + \gamma P\mathcal{H}(\pi_0)) \right) - (I - \gamma P_{\pi_{k+1}})^{-1} \left(\frac{1}{Z_k} (Y_k - \gamma P\mathcal{H}(\pi_{k+1})) \right), \tag{26}
 \end{aligned}$$

where we write $Y_k = \eta_{k+1} q_{k+1} - \eta_0 q_0 + E_{k+1} - X_k$ for the uncluttered notation and the last inequality holds, since $-(I - \gamma P_{\pi_{k+1}})^{-1} P\mathcal{H}(\pi_0) \leq 0$. Next, using the fact that $q_* - q_{\pi_{k+1}} \geq 0$ and rearranging terms, we have

$$\begin{aligned}
 q_* - q_{\pi_{k+1}} &\leq \left| \left((I - \gamma P_{\pi_*})^{-1} - (I - \gamma P_{\pi_{k+1}})^{-1} \right) \frac{E_{k+1}}{Z_k} \right| \\
 &\quad + (I - \gamma P_{\pi_*})^{-1} \left| \frac{1}{Z_k} (\eta_{k+1} q_{k+1} - \eta_0 q_0 - X_k + \gamma P\mathcal{H}(\pi_0)) \right| \\
 &\quad + (I - \gamma P_{\pi_{k+1}})^{-1} \left| \frac{1}{Z_k} (\eta_{k+1} q_{k+1} - \eta_0 q_0 - X_k + \gamma P\mathcal{H}(\pi_{k+1})) \right|. \tag{27}
 \end{aligned}$$

From the assumptions $\|q_k\|_\infty \leq q_{\max}$ for all k , we have $\|X_k\|_\infty = \left\| \sum_{j=0}^k (\eta_{j+1} - \eta_j) T_{\pi_{j+1}|\pi_j}^{\frac{1}{Z_j},0} q_j \right\|_\infty \leq q_{\max} \sum_{j=0}^k |\eta_{j+1} - \eta_j|$. Combined with Eq. (27), we have

$$\|q_* - q_{\pi_{k+1}}\|_\infty \leq \frac{2}{(1-\gamma)Z_k} \left(\left\| \sum_{j=1}^k \eta_j \epsilon_j \right\|_\infty + (\eta_{k+1} + \eta_0 + \sum_{j=0}^k |\eta_{j+1} - \eta_j|) q_{\max} + \gamma \ln |A| \right). \tag{28}$$

Table 1: Hyperparameters of algorithms in deep RL experiments

Parameter	Value
<i>Shared</i>	
optimizer	Adam
learning rate	10^{-4}
discount factor (γ)	0.99
replay buffer size	10^6
number of hidden layers	2
number of hidden units per layer	256
number of samples per minibatch	32
activations	ReLU

Appendix B. Proof of Theorem 3

Define for any $k \geq 0$ the term $q'_k = \lambda_{k+1}(q_k - \ln \pi_k)$. By basic calculus, the evaluation step of Eq. 8 can be transformed as

$$\begin{aligned}
q_{k+1} &= \frac{r}{\lambda_{k+1}} + \ln \pi_{k+1} + \frac{\lambda_k}{\lambda_{k+1}} \gamma P \langle \pi_{k+1}, q_k - \ln \pi_{k+1} \rangle \\
\Leftrightarrow \lambda_{k+1} (q_{k+1} - \ln \pi_{k+1}) &= r + \gamma P \langle \pi_{k+1}, \lambda_k (q_k - \ln \pi_k) \rangle - \lambda_k \langle \pi_{k+1}, \ln \pi_{k+1} - \ln \pi_k \rangle \\
\Leftrightarrow q'_{k+1} &= r + \gamma P \langle \pi_{k+1}, q'_k \rangle - \lambda_k \text{KL}(\pi_{k+1} \| \pi_k). \tag{29}
\end{aligned}$$

For the greedy step, we have

$$\begin{aligned}
\operatorname{argmax}_{\pi} \langle \pi, q_k \rangle + \mathcal{H}(\pi) &\propto \exp(q_k) = \pi_k \exp\left(\frac{q'_k}{\lambda_k}\right) \\
&\propto \operatorname{argmax}_{\pi} \langle \pi, q'_k \rangle + \text{KL}(\pi \| \pi_k). \tag{30}
\end{aligned}$$

Therefore, we have shown that

$$\begin{aligned}
&\begin{cases} \pi_{k+1} = \operatorname{argmax}_{\pi \in \Delta_{\mathcal{A}}^S} \langle \pi, q_k \rangle + \mathcal{H}(\pi) \\ q_{k+1} = \ln \pi_{k+1} + \frac{r}{\lambda_{k+1}} + \frac{\lambda_k}{\lambda_{k+1}} \gamma P \langle \pi_{k+1}, q_k - \ln \pi_{k+1} \rangle \end{cases} \\
\Leftrightarrow &\begin{cases} \pi_{k+1} = \operatorname{argmax}_{\pi \in \Delta_{\mathcal{A}}^S} \langle \pi, q'_k \rangle - \lambda_k \text{KL}(\pi \| \pi_k) \\ q'_{k+1} = r + \gamma P \langle \pi_{k+1}, q'_k - \lambda_k \text{KL}(\pi_{k+1} \| \pi_k) \rangle \end{cases}. \tag{31}
\end{aligned}$$

Appendix C. Hyperparameters

Table. 1 lists the hyperparameters used in the comparative evaluation in Section. 5.

Appendix D. Maze Environment Details

For the tabular experiments, we use randomly generated 5×5 mazes. Figure D shows a sample maze used in the experiment. The agent starts from a fixed position marked with S and can move to any of its neighboring states with success probability 0.9, or to a different random direction with probability 0.1. The agent receives +1 reward when it reaches the goal marked with G , and the environment terminates after 25 steps. The agent cannot enter the black tiles.

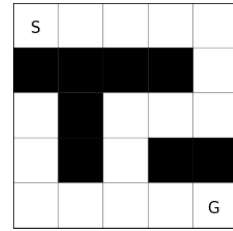


Figure 6: Example of a generated maze.